

Dynamics of Phase Transition Including Quark-Fragment Effects for an Expansion Quark-Gluon Plasma

Li Panlin¹, Wu Hua,² and Xu Mengjie²

¹(Department of Physics, Suzhou Railway Normal College, Suzhou, China)

²(Department of mathematics, Shanghai University, Shanghai, China)

The (1 + 1) dimensional relativistic hydrodynamics equation with a source term including quark-fragment effects is numerically solved and the evolution of energy density, flow rapidity, and baryon number density as the characteristic values of the phase transition possibly produced in nuclear collisions at extreme high energy are also analyzed. The quark-fragment effects in the source term are described by using the phenomenological $SU(3)$ string model with a flavor dynamics.

The numerical results are compared with Kajantie's data. It illustrates indirectly that the results are consistent with the experimental data. The physics picture of our model presented in this paper shows that the phenomenological self-consistent model is reasonable.

Key words: phase transition, quark-fragment effect, evolution.

1. INTRODUCTION

It is well known that a hadron is a bound state of quarks and gluons. This fact has already been proved by using the deep inelastic scattering of a lepton on a hadron. Although no one has yet found

Received on April 8, 1996. Supported by the National Natural Science Foundation of China.

© 1998 by Allerton Press, Inc. Authorization to photocopy individual items for internal or personal use, or the internal or personal use of specific clients, is granted by Allerton Press, Inc. for libraries and other users registered with the Copyright Clearance Center (CCC) Transactional Reporting Service, provided that the base fee of \$50.00 per copy is paid directly to CCC, 222 Rosewood Drive, Danvers, MA 01923.

a free quark at present, the nature of the quarks inside the hadron is understood quite well. People expect to obtain the information about the phase transition of nuclear matter between confinement \leftrightarrow deconfinement by means of studying the production phenomena in the central nucleus-nucleus (A-A) collisions at ultra-relativistic energies ($E_{\text{cm}} \geq 10 \text{ GeV/u}$; $b \approx 0$).

Until now, many methods have been suggested and used to study the properties of the system when phase transition takes place, so as to diagnose whether a new matter phase called the quark-gluon plasma could exist in the process of the phase transition [1].

Because nuclear matter has strong interaction and the non-perturbation treatment related to the confinement phenomena still has not been solved thoroughly, at present all theoretical researches have used phenomenological or semi-phenomenological models to overcome the difficulty of the description of the relativistic light-quark system and the most extensive one used is the relativistic hydrodynamic model. The equations in relativistic hydrodynamics describe the conservation law about the baryon number, energy-momentum, and color charges in the evolution process of the system [2]. According to Bjorken's expansion hydrodynamic model [3], the deconfinement phase transition of the system takes place after the central collisions of the nuclei at the ultra relativistic energy and the degrees of freedom of the system are related to the quarks and gluons. In the range of time $0 \leq t \leq t_0$, due to asymptotic freedom, the interaction is very weak among the excited degrees of freedom. The dynamic behavior of the system is "free flow." Until $t = t_0$, the interaction among the excited degrees of freedom becomes strong enough, so that the local thermal balance is founded in the system and the system begins to flow hydrodynamically. From this time the evolution in time-space can be described by the relativistic hydrodynamic equation $\partial_\mu T^{\mu\nu} = 0$ and the conservation law of the baryon number of the system $\partial_\mu J_B^\mu = 0$ [4]. In a definite initial condition the set of equations can be solved and many of the evolution characters of the system in the quasi-static approximation can be obtained [5].

However, after collisions when the dynamic expansion of the system takes place and the system enters into the state of the relativistic hydrodynamic flow, the internal process in the system is quite complicated. The following two points must be taken into account, i.e., the expansion and the production in the collisions. Therefore the relativistic hydrodynamic equations with a source term must be set up and the flavor dynamics effect (i.e., the quark-fragment effect) should be included in the source term.

2. DESCRIPTION OF THE EQUATIONS AND NUMERICAL METHOD

2.1. Relativistic hydrodynamic equations with the source term

The relativistic hydrodynamic equation with the source term is as follows [6]:

$$\partial_\mu T^{\mu\nu} = \Sigma^\nu, \quad (2.1)$$

$$\partial_\mu J_B^\mu = \sigma, \quad (2.2)$$

where $T^{\mu\nu} = (\varepsilon + p)u^\mu u^\nu - pg^{\mu\nu}$ is the energy-momentum tensor of the system, $J_B^\mu = n_B u^\mu$ is the flow density of the baryon number, $u^\mu = \gamma(1, \boldsymbol{v})$ is the four-dimensional velocity which degenerates into two dimensions in this paper, ε , p are the energy density and local pressure of the system, respectively, $\gamma = [1 - v^2]^{-1/2}$ is the Lorentz factor and $g^{\mu\nu}$ is the gauge tensor.

The evolution of the system is described by means of the energy density $\varepsilon(x, t)$, the baryon number density $n_B(x, t)$, and the flow velocity $v(x, t)$. The local pressure, energy density, and the baryon number density are related by the equation of state $p = p(\varepsilon, n_B)$.

In the Eqs. (2.1) and (2.2), the light-cone coordinates are used as

$$x^\pm = t \pm x, \quad \tau = (x^+ x^-)^{\frac{1}{2}} = (t^2 - x^2)^{\frac{1}{2}}, \tag{2.3}$$

and then further transformation of the variables is made and they will have simple Lorentz invariant properties as

$$\begin{cases} \hat{t} = \log \left[\frac{\tau}{\tau_0} \right] = \frac{1}{2} \log \left[\frac{x^+ x^-}{\tau_0} \right], \\ y = \frac{1}{2} \log \left[\frac{x^+}{x^-} \right]. \end{cases} \tag{2.4}$$

At the same time, the source terms Σ, σ are combined linearly as

$$\begin{cases} \Sigma^0 \cosh \theta - \Sigma^1 \sinh \theta, \\ -\Sigma^0 \sinh \theta + \Sigma^1 \cosh \theta. \end{cases} \tag{2.5}$$

Equations (2.1) and (2.2) are joined and rewritten as

$$\begin{cases} (\partial_i + \bar{v}\partial_y)\varepsilon + (\varepsilon + p)(\bar{v}\partial_i + \partial_y)\theta = \frac{e^i}{\cosh(\theta - y)} (\Sigma^0 \cosh \theta - \Sigma^1 \sinh \theta), \\ (\bar{v}\partial_i + \partial_y)p + (\varepsilon + p)(\partial_i + \bar{v}\partial_y)\theta = \frac{e^i}{\cosh(\theta - y)} (-\Sigma^0 \sinh \theta + \Sigma^1 \cosh \theta), \\ (\partial_i + \bar{v}\partial_y)n_B + n_B(\bar{v}\partial_i + \partial_y)\theta = \frac{e^i}{\cosh(\theta - y)} \sigma, \end{cases} \tag{2.6}$$

The initial conditions are taken as

$$\varepsilon(y, \hat{t} = 0) = 0; \quad \theta(y, \hat{t} = 0) = y; \quad n_B(y, \hat{t} = 0) = 0, \tag{2.7}$$

where

$$\bar{v} = \bar{v}(y, \hat{t} = 0) = \tanh(\theta - y). \tag{2.8}$$

In order to determine Σ^i and σ , a summation is performed with respect to all collisions (in the region of $0 \leq t' \leq d_i$) [6]

$$\sum_{\text{all collisions}} = N_A \equiv n_0 2R_A = n_0 \sinh y_B^* \int_0^{d_i} dt',$$

where A is the nuclear number of the colliding nuclei and $A = 238$ is taken in this paper. We obtain

$$\begin{aligned} \alpha(x, t) &= n_0 \sinh y_B^* \int dt' \rho_N \left[\frac{1}{2} \log \left(\frac{t - t' + x}{t - t' - x} \right) \right] 2\delta[(t - t')^2 - x^2 - 1] \\ &= n_0 \sinh y_B^* \rho_N [\log(\sqrt{x^2 + 1} + x)] \frac{1}{\sqrt{x^2 + 1}} \Theta(x, t), \end{aligned}$$

and similarly

$$\begin{aligned}\Sigma^0(x, t) &= n_0 \sinh y_B^* \sum_i \bar{m}_i \rho_i [\log(\sqrt{x^2 + 1} + x)] \Theta(x, t), \\ \Sigma^1(x, t) &= \frac{x}{\sqrt{x^2 + 1}} \Sigma^0(x, t),\end{aligned}$$

where the step function is as

$$\Theta = \begin{cases} 1, & \text{in the region of source} \\ 0, & \text{out of the region of the source} \end{cases}$$

The source terms of the equations, Σ^0 and σ , describe how the hadron particles are produced and how they enter the hydrodynamic expansion stage in the system.

2.2. Treatment of the source terms of the equations and the flavor dynamics of quark-fragment effect

The expression of the source terms in the equations can be found in Ref. [6]. In order to take into account the quark-fragment effects in the process of confinement \leftrightarrow deconfinement phase transition sufficiently, the phenomenological $SU(3)$ string model [7] is used to ensure the self-consistence of the theoretical treatment in this paper.

In the lowest order perturbation QCD, there are two kinds of reactions which can change the chemical constituents of the quark-gluon plasma:

$$\begin{cases} g + g \rightarrow q + \bar{q}, [g \quad q], \\ q_1 + \bar{q}_1 \rightarrow q_2 + \bar{q}_2, [q \quad q]. \end{cases} \quad (2.9)$$

According to $SU(3)$ flavor-dynamics, there are three possible flavors for quarks, then in the above-mentioned reactions the three different flavors should be included, respectively. They are:

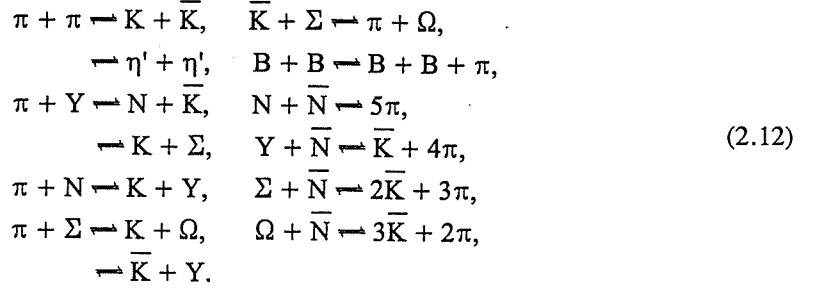
$$[gu, gd, gs; ud, us, ds].$$

As the system volume of the quark-gluon plasma is continuously expanding, the non-perturbative treatment must be applied. When the volume is expanding, the distance between the quarks becomes so large that the quarks feel the action of confinement force. Specially in the picture of the string model, the string between the neighboring $q\bar{q}$ is formed. As the string length grows the confinement force is also grows. Finally, the old string (quark pair) is broken to create two new strings. Depending on how much energy the new strings have, they would either form a hadron or continue to remain in the quark-gluon plasma phase. Therefore, the following processes are considered simply:

$$\begin{aligned} q_1 \bar{q}_2 &\rightarrow q_1 \bar{q}_3 \bar{q}_3 \bar{q}_2, \\ &\rightarrow (q_1 \bar{q}_3) q_3 \bar{q}_2, \\ &\rightarrow q_1 \bar{q}_3 (q_3 \bar{q}_2), \\ &\rightarrow (q_1 \bar{q}_3) (q_3 \bar{q}_2). \end{aligned} \quad (2.10)$$

$$\begin{aligned} q_1 \bar{q}_2 \bar{q}_3 &\rightarrow q_1 q_2 \bar{q}_4 \bar{q}_4 \bar{q}_3, \\ &\rightarrow (q_1 \bar{q}_2 q_4) q_4 \bar{q}_3, \\ &\rightarrow q_1 \bar{q}_2 - q_4 (\bar{q}_4 q_3), \\ &\rightarrow (q_1 q_2 q_4) (\bar{q}_4 q_3). \end{aligned} \quad (2.11)$$

where the bracket notation $(q\bar{q})$ is a configuration of meson and $(qq\bar{q})$ is a configuration of the baryon. After the hadrons are formed, they do not escape from the system at once, but the collisions and reactions still take place among the hadrons and the flavor components are further changed. Only hadron particles with mass $m_i \leq 2$ GeV are considered in this paper, thus the possible recombination reaction modes are



To join the equation of energy change of the system, the balance relation of the pressure [7]

$$\frac{d}{dt} \sum_i \beta_i V \varepsilon_i(n_i, T) = -p \frac{d}{dt} V, \tag{2.13a}$$

$$\frac{d}{dt} \sum_i \phi_i p_i(n_i, T) = 0 \tag{2.13b}$$

and the rate equation of particle number change describing the quark chemical dynamics

$$V \dot{n}_i = \dot{N}_i - n_i (\dot{\beta}_i V + \beta_i \dot{V}), \tag{2.13c}$$

a coupling equation set is obtained

$$\begin{cases} A\dot{\beta} + B\dot{T} = C, \\ D\dot{\beta} + E\dot{T} = F, \end{cases} \tag{2.14}$$

The details of the derivation of the above-mentioned equations can be found in Ref. [7].

The time-space evolution of the energy density, the pressure, and the number density of various hadron particles of the system can be obtained after numerical solution. The calculations in details can be found in Ref. [8]. Figure 1 shows a typical numerical result, $\rho_i(x, t)$ in the source term can be calculated by means of $SU(3)$ flavor dynamics from the Eqs. (2.13). Now the source terms on the right-hand side of Eq. (2.6) are obtained and the equation set (2.6) can be solved numerically.

2.3. Numerical method of solution

For the first two equations in Eq. (2.6), the implicit differential scheme with a small stickiness term is used. Then the Newton's and the fastest descending methods are jointly used, so as to ensure the convergence and its acceleration in the calculation. The third equation in Eq. (2.6) is solved by using a backward-differential scheme on the variable \hat{t} and a forward-differential left-deflect differential scheme on the variable y .

3. NUMERICAL RESULTS AND DISCUSSION

First, Eq. (2.6) is solved numerically at $y = 2y_B^* = 6.8$ for the central collisions of the U + U system and in the central rapidity region the observed value of rapidity densities of hadron particles

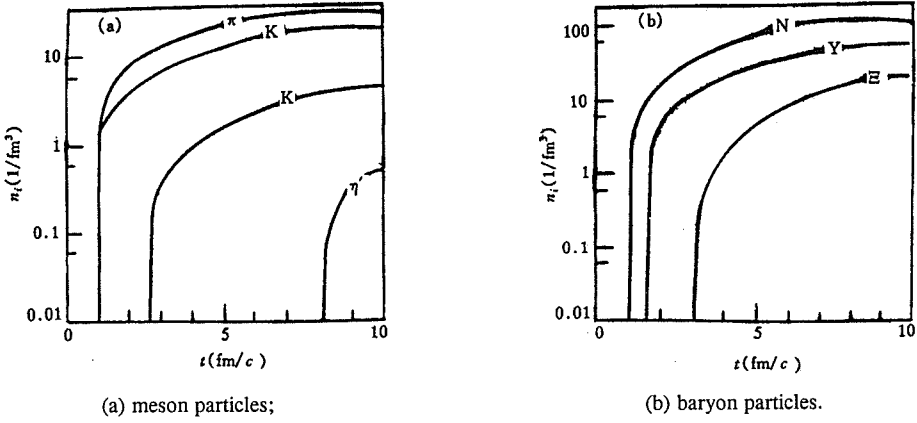


Fig. 1

The evolution curve of the hadron particle densities.

Initial volume $V_0 = 100 \text{ fm}^3$, initial density of the baryon number

$n_B^{(0)} = 0.63 \text{ fm}^{-3}$ and initial temperature $T_0 = 180 \text{ MeV}$.

are directly used to express the production rate of hadrons (only two kinds of the hadrons: meson π and nucleon N are included) [6].

$$\begin{cases} \rho_\pi(y) = \rho_0(1 - x_\pi)^n = \rho \left(-\frac{\bar{m}}{m_N} \frac{\cosh y}{\cosh y_B^*} \right)^n, & n = 3, \\ \rho_N(y) = \frac{\cosh y}{\sinh y_B^*}, \end{cases} \quad (3.1)$$

where

$$\rho_0 = 2.4, \quad \bar{m}_\pi = (m_\pi^2 + \langle P_T^2 \rangle_\pi)^{\frac{1}{2}} = 0.5 \text{ GeV}$$

They are introduced to express the particle rapidity densities in the source terms Σ^0 , Σ^1 , and σ of Eq. (2.6). The calculation results are shown in Fig. 2. It has well reproduced the results in Ref. [6]. Comparing our results with the results in Ref. [6], it can be seen that the trend and the order of magnitude of the two numerical solutions (isograms) are basically in agreement. Thus the numerical test show clearly the convergence and efficiency of this numerical method of the solution.

Based on the above-mentioned numerical test, the calculated ρ_i and ρ_N based on the theoretical model of $SU(3)$ flavor dynamics are put in the source terms, Σ^0 , Σ^1 , and σ , of the Eq. (2.6). In the flavor dynamics calculation the only hadron particles with mass $m_i \leq 2 \text{ GeV}$ are taken into account, so that the mesons are π , K , \bar{K} , and η' and the baryons are N , Y , and Ξ , respectively. Then the equations set (2.6) are again solved numerically. The calculated results are shown in Fig. 3.

To compare our results with the results in Ref. [6] the distribution trend and order of magnitude of curves of equal flow-rapidity and the rapidity density of equal baryon-number are all consistent except for the curve of equal energy-density. When comparing our curve of equal energy-density with the curve in Ref. [6], one can easily find that the calculated result in this paper shows that the maximum

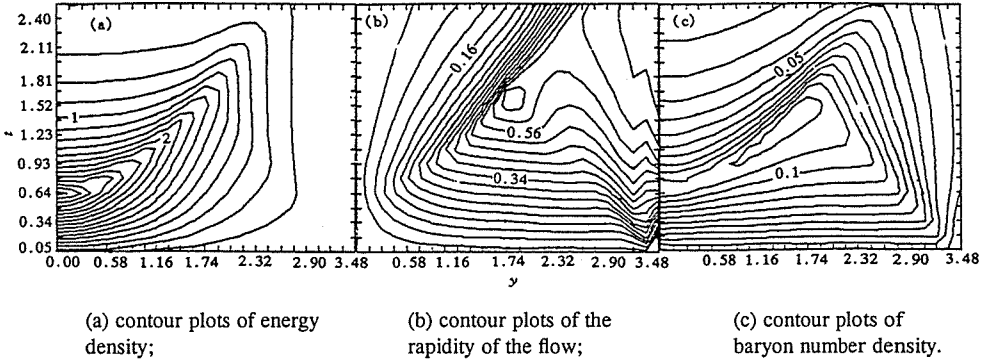


Fig. 2

For $y = 2y_B^* = 6.8$, the U+U central collision, the production rate of hadrons in the source terms, Σ^0 , Σ^1 , and σ , of Eq. (2.6) is the observed values of the particle densities taken from Ref. [6] and only two kinds of particles are included: π -meson and N-nucleon.

value of energy density $\epsilon_{\max} \approx 3.8 \text{ GeV}/\text{fm}^3$ is at $y = 1.5$, instead of at $y = 0$ as in Ref. [6]. In order to further investigate the problem, we also take only two terms of the theoretical value of the particle rapidity density in the source terms, i.e., ρ_π and ρ_N , in order to be consistent with Kajantie's calculation condition. The calculated results are shown in Fig. 4. From the curve of distribution of iso-energy density in Fig. 4(a) it can be found that the $\epsilon_{\max} \approx 1.5 \text{ GeV}/\text{fm}^3$ is at $y \approx 1.5$ and not at $y = 0$. On this difference, we think that in the investigated system of quark-gluon plasma, at the first moment, the system is really in an extreme contraction condition and at that time the energy density of the system is at the maximum, but our attention is not focused here. Afterwards, as the system expands, the following reactions take place because quarks and gluons are carrying a lot

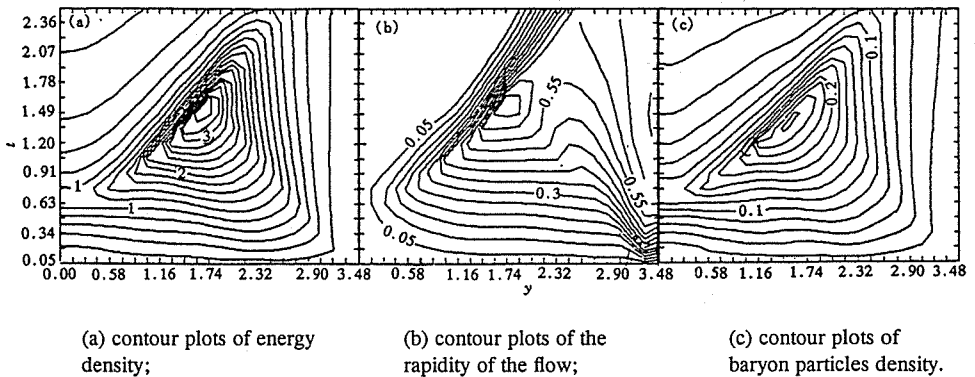


Fig. 3

For U + U central collision at $y = 2y_B^* = 6.8$, the production rate of hadrons in the source terms Σ^0 , Σ^1 , and σ of Eq. (2.6) is the theoretical value which is calculated by the flavor dynamics of SU(3) string model and the produced hadron particles with mass $m_i \leq 2 \text{ GeV}$ are included.

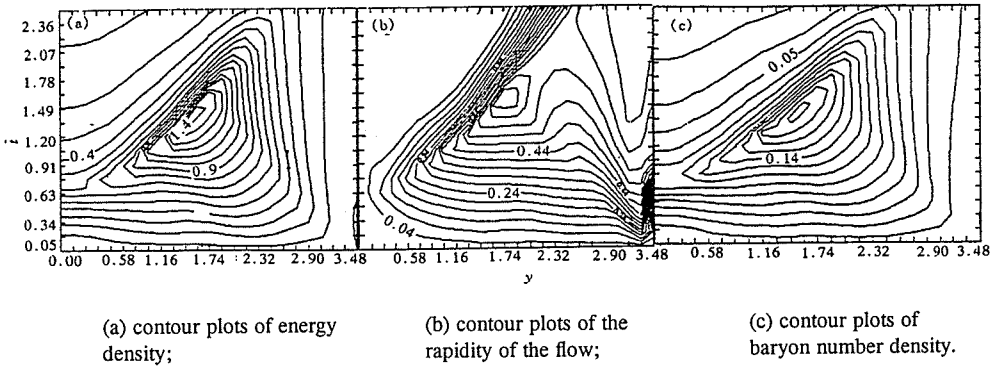


Fig. 4

The condition is the same as in Fig. 3, but the theoretical values of the hadron particles are only two kinds: that of the π -meson and that of the N-nucleon.

of energy and colliding with each other:

$$q + q \rightleftharpoons q + \bar{q}, \quad q_1 + \bar{q}_1 \rightleftharpoons q_2 + \bar{q}_2.$$

Undergoing continuous expansion, according to the theory of the string model, the breaking of the strings listed in the Eqs. (2.10–2.12) and various possible recombination reactions by the rule of the flavor dynamics take place. In the above two steps, the expansion of the fluid, continuous collisions among quarks and gluons and also the breaking of the string (i.e., quark-fragment), each of these factors causes energy of the system to be continuously consumed so that the energy density becomes smaller and smaller. However, once the recombination reaction among quarks take place by the flavor dynamics and afterwards when the hadron particles are "frozen," a lot of reaction energy is released so that the energy density of the system increases. At the same time, some amount of "frozen" hadron particles escape from the system. From the production of hadron particles and even from their "frozen" state to the particle emission of their final state, there is a "very long" physical process, e.g., the re-collision of hadron particles and the flavor recombination which are both described in Eq. (2.12). This is the only physical content about evolution in the system which is described by us, which is different from that in Ref. [6] where the observed rapidity densities of the final state of particles are directly used as equal to the rapidity densities of hadron particles which are produced in the hadronization process of the system (which is shown in the source term of the equation), such a simple correlation has not considered the gradual evolution of the system.

In addition, the comparison between the corresponding rapidity density curves of equal flow-rapidity and the equal baryon-number shows that their maximum is really at about $y = 1.5$ and not at $y = 0$ even in Kajantie's results [6]. We think that the identity of characters could be taken as a collateral evidence of the above-mentioned argument because the difference in the points of view on the evolution of the system could easily produce different results in numerical solutions of the equation group.

Considering various possible initial conditions of the physics problem the following initial values are also applied:

$$\varepsilon(y, \hat{t} = 0) = 0.01; \quad \theta(y, \hat{t} = 0) = y; \quad n_B(y, \hat{t} = 0) = 0$$

The calculation results show that the change of the solution is small when the initial value has small change, which shows that the differential scheme used in this paper has a certain stability.

In summary, in this paper a self-consistent theoretical method is presented, in which the relativistic hydrodynamics is used to describe phase transition process of an expanding quark-gluon plasma and the quark-fragment effect is also considered at the same time.

REFERENCES

- [1] K. Kajantie and H.I. Miettinen, *Z. Phys.*, **C9**(1981), p. 341; L.P. Csernai, *Phys. Rev.*, **D29**(1984), p. 1945; C. Cale and J. Kapusta, *Nucl. Phys.*, **A471**(1987), p. 350.
- [2] S.A. Chin, *Phys. Lett.*, **78B**(1978), p. 552.
- [3] D. Bjorken, *Phys. Rev.*, **D72**(1983), p. 140.
- [4] L.L. Rozental, *Sov. Phys. UPS.*, **18**(1975), p. 430.
- [5] G. Baym *et al.*, *Nucl. Phys.*, **A407**(1983), p. 541.
- [6] K. Kajantie, R. Ratio, and P.V. Ruuskanen, *Nucl. Phys.*, **B222**(1983), p. 152.
- [7] H.W. Barz *et al.*, *Nucl. Phys.*, **A484**(1988), p. 661.
- [8] Shi Xinhui, master's thesis (in Chinese), Dept. of Math., Shanghai Univ., (1993).
- [9] D. Potter, *Computational Physics*, London: John Wiley & Sons, (1973), p. 67.